AAPS PharmSciTech, Vol. 19, No. 5, July 2018 (© 2018)
DOI: 10.1208/s12249-018-1062-8

Research Article

Transient Temperature Monitoring of Pharmaceutical Tablets During Compaction Using Infrared Thermography

Hwahsiung P. Lee,[1] Yuriy Gulak,[1] and Alberto M. Cuitino[1,2]

Received 14 February 2018; accepted 7 May 2018; published online 4 June 2018

Abstract. Manufacturing of pharmaceutical tablets from powders is always accompanied by the conversion of irreversible mechanical work of compaction into heat. The heat is generated due to friction between powder particles, particles and the die wall, plastic deformation of particles, bonding, and other irreversible processes. The resulting temperature increase potentially might have significant effects on a tablet's mechanical properties, disintegration time, and drug release. In the present work, we show that using infrared thermography as a nondestructive and noncontact process analytical technology (PAT) tool to measure the tablet's rate of cooling, in contrast to the temperature evolution, can be directly related to the tablet's thermal diffusivity. Results show the potential capabilities of this technique to discriminate and toward predicting tensile strength of tablets between same formulations produced at same compaction force but experienced different process shear conditions. Correlation of the tablet's tensile strength, relative density, and rate of cooling at *regular regime* with respect to different process shear is also discussed.

KEY WORDS: tablet transient temperature; infrared thermography; regular regime; process shear; tensile strength.

INTRODUCTION

Manufacturing of a pharmaceutical tablet from powder is always accompanied by the conversion of irreversible mechanical work of compaction into heat. The heat is generated due to friction between powder particles, particles and the die wall, plastic deformation of particles, bonding, and other irreversible processes (1). The resulting temperature increase potentially might have significant effects on the tablet's mechanical properties, disintegration time, and drug release (2). Temperature increase during compaction of pharmaceutical powder has been of interest to pharmaceutical scientists: studies such as using thermocouples imbedded in the compressed tablet to measure the temperature changes (3,4), utilizing infrared thermoviewer to monitor tablet surface temperature (1,5,6), and finite element analysis for modeling temperature and density distribution within the pharmaceutical tablet (7). Influence of temperature on mechanical properties of the tablet has been investigated by some studies (8,9). The surface characteristics changes during sheared mixing of heterogeneous systems can affect powder and tablet properties (10,11). Temperature rise also affects the physicochemical properties of the medicinal substances, including chemical stability, crystallinity, and polymorphous state (12). The temperature increase in the powder during compaction is detrimental to heat-sensitive active pharmaceutical ingredients (APIs) with low heat conductivity, such as most organic materials used in pharmaceutical formulations. Therefore, it is important to understand the thermomechanical behavior of powders during compaction.

Among several techniques of tablet temperature measurement directly after the tablet's ejection from a tablet press, infrared thermography has the unique advantages (1,5,6), to be utilized as a potential in-line process analytical technology (PAT) tool for quality control. This technique, being nondestructive and noncontact, allows accurate tablet's surface temperature field acquisition in real time. The primary source of infrared radiation is heat. Infrared camera can capture heat signature of pharmaceutical tablets and convert the information for further data analysis.

There are challenges in finding efficient characterization of the variability in formulations and manufacturing processes during production of tablets in order to provide adequate product quality control. We are addressing these challenges (i) by demonstrating infrared thermography as a potential nondestructive and noncontact PAT tool is suitable to evaluate thermal properties of the tablet during compaction process and (ii) by showing infrared thermography can be used to differentiate tablets of the same formulation compacted at the same compaction force but experienced different process shear conditions and correlate to tablet mechanical properties. In the present work, we show that the

[1] Department of Mechanical and Aerospace Engineering, Rutgers University, 98 Brett Rd., Piscataway, New Jersey 08854, USA.
[2] To whom correspondence should be addressed. (e–mail: cuitino@gmail.com)

tablet's rate of cooling, in contrast to the temperature evolution, can be directly related to tensile strength of the tablet. Results show the potential capabilities of this technique to discriminate between same formulation tablets produced at same compaction force but experienced different process shear conditions.

MATERIALS AND METHODS

Materials

In the current study, lactose (monohydrate N.F., crystalline, 310, regular, Foremost Farms, Rothschild, WI, USA), acetaminophen (APAP; semi-fine crystalline powder, USP/paracetamol PhEur, Mallinckrodt, Raleigh, NC, USA), and magnesium stearate N.F. (MgSt; non-Bovine, Tyco Healthcare/Mallinckrodt, St. Louis, MO, USA) were employed as the test and lubricant materials.

To investigate the effect of different process shear that the powder blend might have experienced during continuous tablet manufacturing operation (13), three cases of batch production were considered. In case 1 (hereafter referred to as No Additional Shear, NAS), lactose (90%, *w*/*w*) and APAP (9%, *w*/*w*) were blended for 15 min at 15 rpm in a Twin Shell V-Blender (Patterson-Kelley, East Stroudsburg, PA) and then mixed for additional 2 min at 15 rpm after MgSt was added. In case 2 (hereafter referred to as 160 Rev sheared), the blended powder from case 1 was unloaded from the V-blender and subjected to a controlled shear environment in a modified Couette Cell (MCC, Metropolitan Computing Corporation, East Hanover, NJ, USA) at a shear rate of 80 rpm for 2 min. In case 3 (hereafter referred to as 640 Rev sheared), the blended powder from case 1 was unloaded from the V-blender and subjected to a shear rate of 80 rpm for 8 min in the modified Couette Cell. The total blend time of NAS, 160 Rev sheared, and 640 Rev sheared cases was 17, 19, and 25 min respectively. All measurements were conducted at ambient conditions of 22 ± 3°C and 30 ± 5% RH. Because of the lack of means to access shear rates in a V-blender and therefore estimate the exposure to total shear, mixing time has been the only variable correlated in the literature with blend and tablet properties. The advantage of modified Couette Cell designed with equidistant interlocking pins is that it provides a nearly uniform shear environment in the whole cell (10,14,15). The choice of lactose-APAP formulation is for proof of concept to suggest feasibility of using infrared camera as a characterization tool of manufacturing steps. We have initially selected lactose since it is a more revealing case as the thermal signature is weak due to low plastic deformation resulting in heat. Additional testing is required for standardized modeling.

Methods

Tablet Compaction

The blends were compressed using a tablet press (Presster, Metropolitan Computing Corporation, East Hanover, NJ) to simulate a Fette PT 2090 IC, 36 stations press with a press speed of 20 rpm. A dwell time of 22.1 ms (*i.e.*, the time when the flat portion of the punch head was in contact with the compaction roll) was corresponding to a production speed of 43,200 tablets per hour. The ejection angle was set at 5.3°. No pre-compression was used. A set of flat-faced punches, 10-mm diameter, was used to produce 350-mg tablets.

Infrared Thermography

A calibrated infrared camera (ICI Model 7320, Infrared Cameras Inc., Beaumont, TX) was utilized to evaluate the temperature evolution on the whole surface area of the tablet after the tablet's ejection from the tablet press. The camera was placed at a distance about 18~20 cm perpendicular right above the tablet. All measurements were conducted at ambient conditions of 22 ± 3°C and 30 ± 5% RH.

Infrared Image Processing and Analysis

The thermal images of tablet temperature were converted to comma separated values (CSV) files for data processing.

Tablet Tensile Strength

The tensile strength of tablets, σ_t, is given by:

$$\sigma_t = \frac{2F}{\pi D t}$$

where F is the breaking force and D is the diameter of the tablet, which is assumed to be constant and equal to 10 mm as radial relaxation was minimal; t is the thickness of the tablet (16).

RESULTS AND DISCUSSION

Nondestructive and Noncontact Infrared Thermography on Pharmaceutical Tablets

Figure I shows the infrared thermography of the whole surface area of tablets that were manufactured with the same formulation but subjected to different process shear conditions and compacted at compaction force of 24 ± 0.5 kN, 20 ± 0.5 kN, and 16 ± 0.5 kN. There is instantaneous real-time visible difference in the infrared thermography to differentiate tablets that experienced different process shear.

Tablet Temperature *vs* Time Profiles

Figure II illustrates the time evolution of the maximal temperature on the top surface of the tablets after being ejected from the die. The tablets are manufactured using the same compaction force, but the blends are subjected to three different process shear conditions. The result demonstrates strong sensitivity of measured temperature profiles to the powder process shear conditions. The result shows that with same compaction force during compaction of tablets, the lesser sheared powder blend exhibits distinguishably higher measured tablet surface temperatures. It is worth noting that the tablet temperature difference between sheared and unsheared powders reflects the change in physicochemical behavior of the particle surface as a result of process shear.

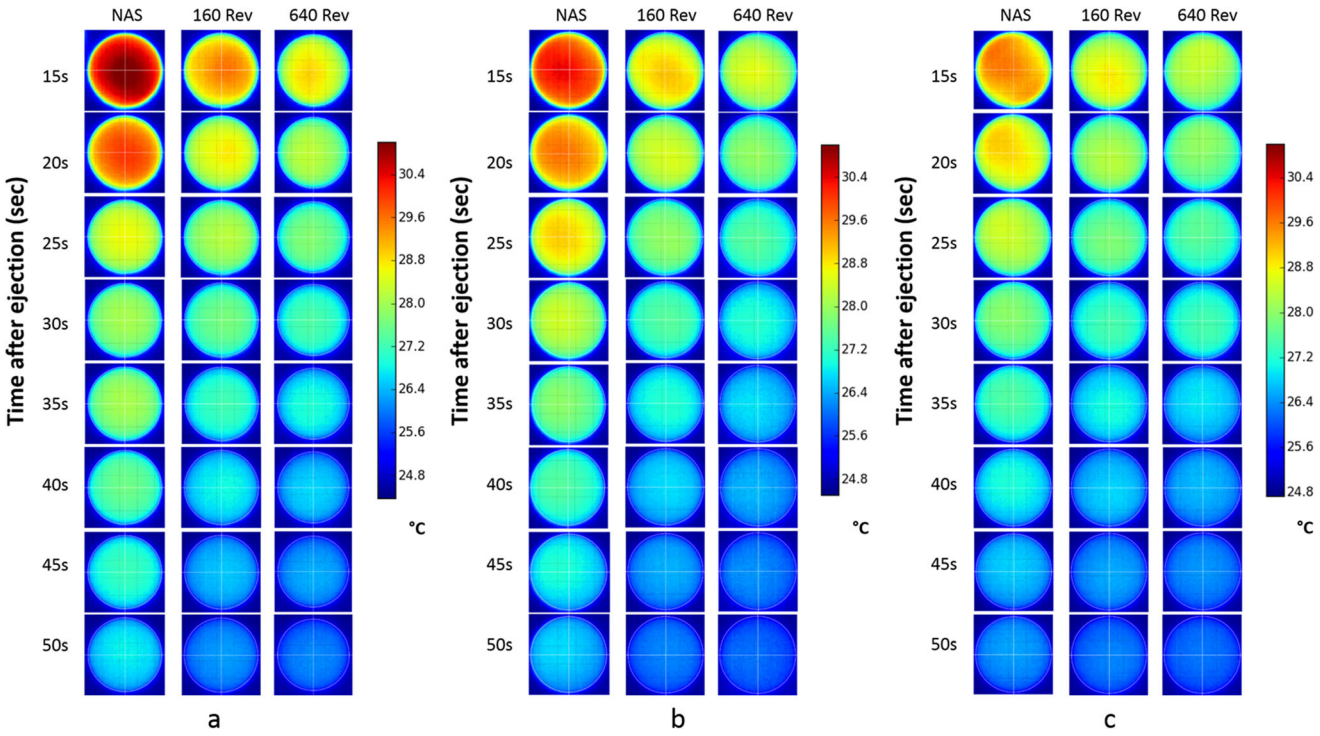

Fig. I. Infrared thermography of tablets with the same formulation but subjected to different process shear (No Additional Shear (NAS), 160 Rev sheared, and 640 Rev sheared) compressed at (**a**) 24 ± 0.5 kN, (**b**) 20 ± 0.5 kN, and (**c**) 16 ± 0.5 kN

This significant difference in tablet temperature can be attributed to the deposition of thin layers of lubricant (MgSt) film on the surface of powder particles (10). It is also possible that the change in surface energies of powder particles due to process shear alters the contact mechanics between adjacent particle surfaces and the pattern when these powder particles rearrange under compaction thus changing the tablet temperature. Utilizing infrared camera to measure tablet temperature in real time can provide a calibrated temperature profile for manufacturing quality control during continuous tablet manufacturing operation. In addition, collected temperature distribution data can be used to determine the tablet thermal diffusivity among other parameters, which is related to a tablet's pore microstructure formed during compaction. The information of tablet surface temperature with

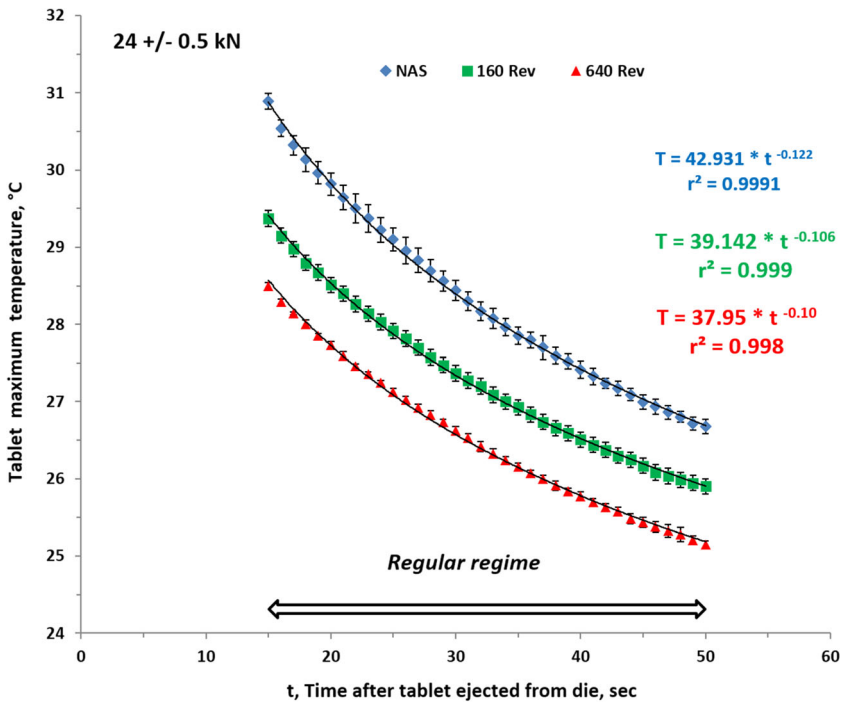

Fig. II. Tablets compacted at 24 ± 0.5 kN with No Additional Shear (NAS), 160 Rev sheared, and 640 Rev sheared powder blends

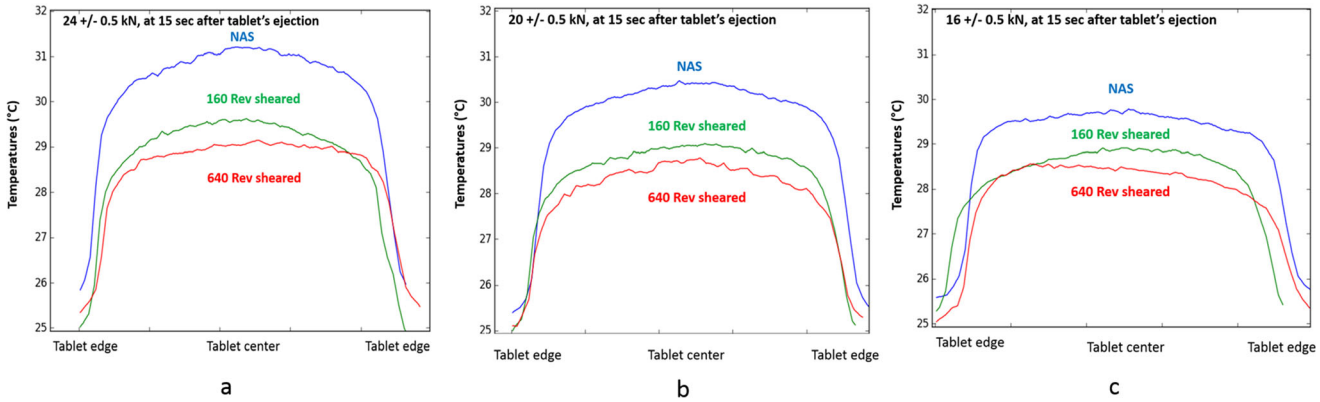

Fig. III. Temperature profile of tablets (view from above the tablet) from edge to edge at 15 sec after ejection from the die with the same formulation but subjected to different process shear (No Additional Shear, NAS (blue), 160 Rev sheared (green), and 640 Rev sheared (red)) compressed at (**a**) 24 ± 0.5 kN, (**b**) 20 ± 0.5 kN, and (**c**) 16 ± 0.5 kN

progression of time also allows us to estimate the initial tablet temperature immediately after the compaction. The estimated initial tablet temperature immediately after the compaction with 24 ± 0.5 kN compaction force for NAS is ~ 42.9°C, for 160 Rev sheared is ~ 39.1°C, and for 640 Rev sheared is ~ 37.9°C.

Figure III shows the tablet surface temperature profile from the left edge to the right edge of the tablet at 15 sec after the tablet's ejection from the die with compaction force of 24 ± 0.5 kN, 20 ± 0.5 kN, and 16 ± 0.5 kN for all three different process shear conditions. There is a clear distinction that less sheared formulation has higher tablet surface temperature. For example, in Fig. III(a), tablets compacted with 24 ± 0.5 kN, at 15 sec after ejection from the tablet press, the maximum temperature recorded near the center of tablet is ~ 31.2°C for NAS case, ~ 29.6°C for 160 Rev sheared case, and ~ 29.1°C for 640 Rev sheared case. This is a significant indication of heat generated during compaction at the particle interface due to frictional interactions between moving powder particles and within the particles due to irreversible deformation. More heat is generated with less sheared formulation like the NAS case which has less evenly distributed MgSt as lubricant among excipient particle surface. On the contrast, less heat exhibits more uniformly distributed lubricant on 160 Rev sheared and 640 Rev sheared cases. Figure IV shows the cooling process of tablet surface temperature with the progression of time from the left edge to the right edge of the tablet of NAS, 160 Rev sheared, and 640 Rev sheared cases compacted at 24 ±0.5 kN.

Regular Regime

Consider cooling of a homogeneous body having the initial temperature $T_i(x, y, z, t)$, which is put in the surroundings of the constant temperature T_{env}, with a constant surface heat transfer coefficient. The solution of the corresponding heat conduction problem is:

$$T_i(x, y, z, t) - T_{\text{env}} = \sum_{n=1}^{\infty} c_n \varphi_n(x, y, z) e^{-m_n t} \tag{1}$$

where c_n are constant coefficients; the factors $\varphi_n(x, y, z)$ are functions of coordinates only. Note that the eigenvalues m_n are positive and satisfy the inequality $m_1 < m_2 < \ldots < m_n < \ldots$ Thus, higher order terms of the series in Eq. (1) rapidly decrease with time and at a certain moment of time can be neglected. The temperature field is then described by the first dominant term in Eq. (2):

$$T_i(x, y, z, t) - T_{\text{env}} \approx c_1 \varphi_1(x, y, z) e^{-m_1 t} \tag{2}$$

which indicates that regular cooling is established. The function $\varphi_1(x, y, z)$ does not depend on initial conditions;

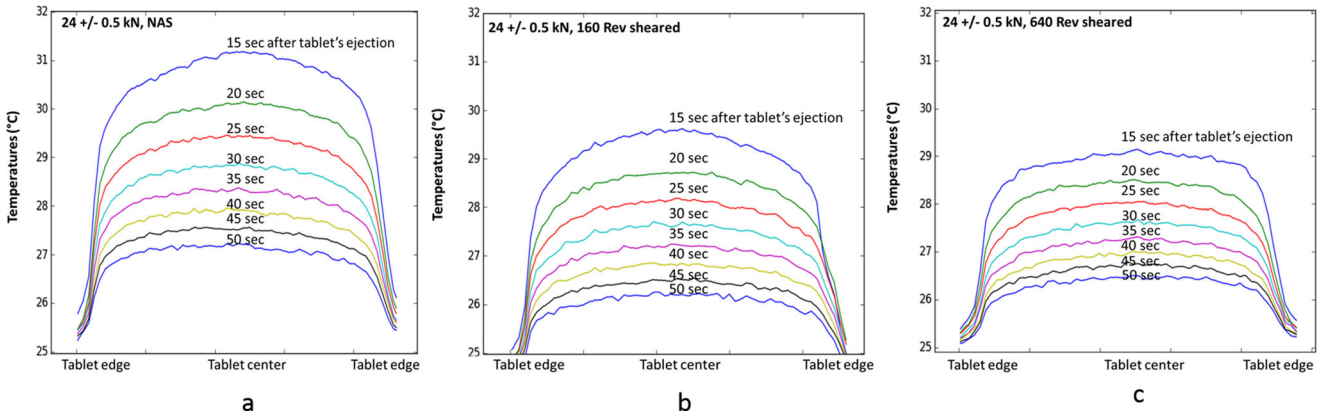

Fig. IV. Temperature profile as time progress (15 ~ 50 sec, view from above the tablet) from edge to edge of the tablet compressed at 24 ± 0.5 kN of (**a**) No Additional Shear (NAS), (**b**) 160 Rev sheared, and (**c**) 640 Rev sheared

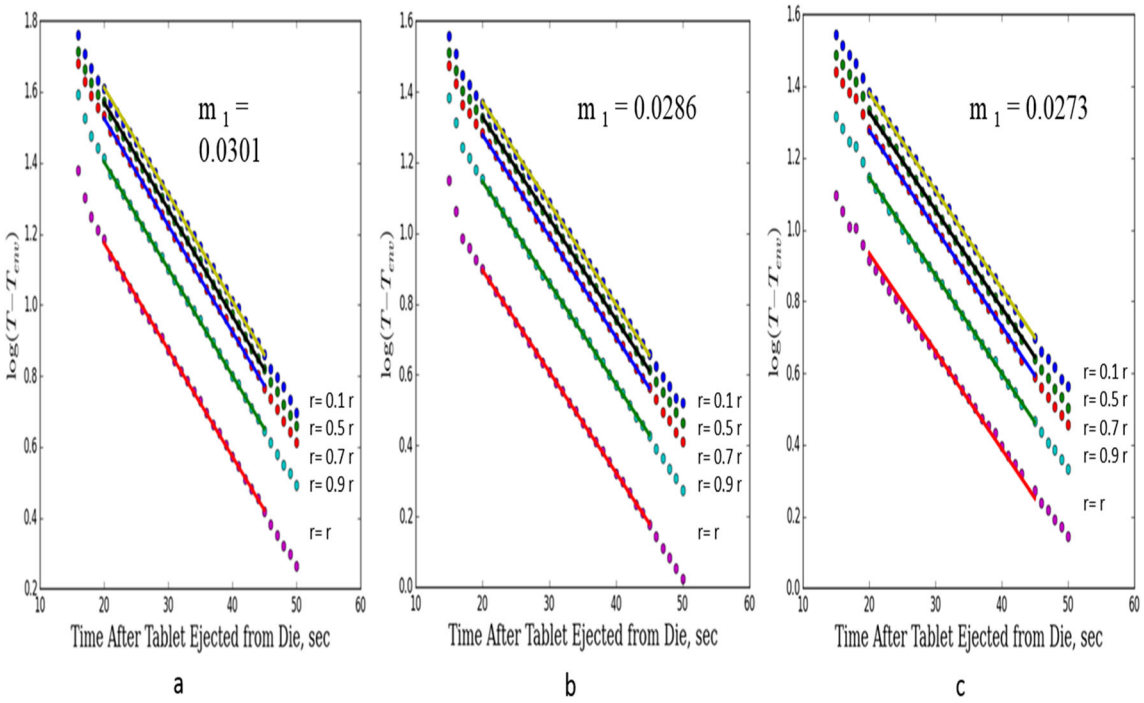

Fig. V. log (*T*−*T*env) *vs* time (*i.e.*, slope, m_1) after the tablet was ejected from the die at location of $r = 0.1r$, $0.5r$, $0.7r$, $0.9r$, and r of tablet compressed at 24 ± 0.5 kN of (**a**) No Additional Shear (NAS), (**b**) 160 Rev sheared, and (**c**) 640 Rev sheared

therefore, the regular cooling process is fully determined only by the boundary conditions and the physical properties of the body. Taking the logarithm of Eq. (2) yields Eq. (3):

$$\log(T_i(x,y,z,t) - T_{\text{env}}) = -m_1 t + \log(c_1 \varphi_1(x,y,z)) \tag{3}$$

Equation (3) shows that the logarithm of excess temperature changes linearly in time at all points of the body. Moreover, the slope of such linear functions m_1 is the same for all points and is called the *rate of cooling*.

Summarizing, the entire cooling process can be divided into two stages. The first *transient* stage is characterized by the strong dependence of the initial temperature distribution, and the temperature evolution is described by Eq. (1). The second stage is the *regular regime* (17–19), described by Eq. (2).

It should be noted that the pharmaceutical tablets are in general heterogeneous; thus, the spatial variability of the cooling rate in the regular regime might be expected. Experimental results, however, indicate close values for the fitted slopes evaluated at different points on the tablet's surface as shown in Fig. V for NAS, 160 Rev sheared, and 640 Rev sheared blends compacted at 24 ± 0.5 kN.

In Fig. VI, we present the relationship between the average slope of log $(T - T_{env})$ *vs* time, m_1, and relative density, $\overline{\rho}$, of

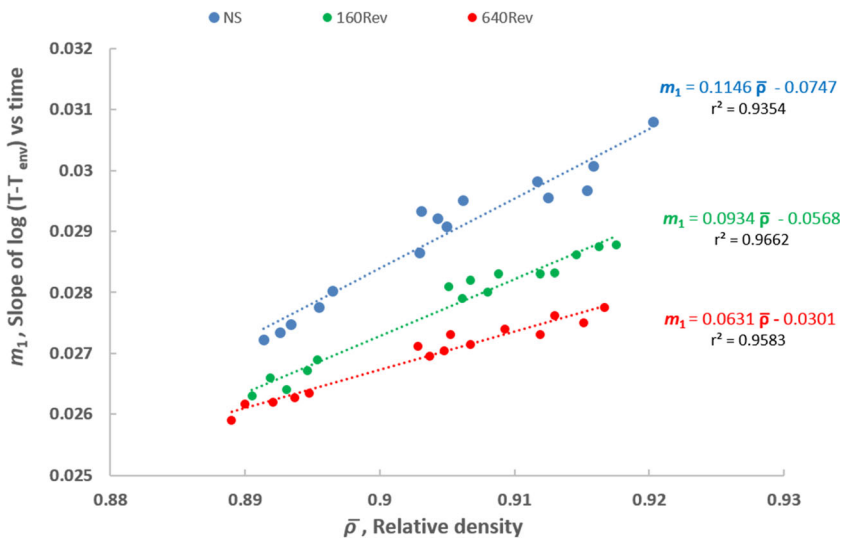

Fig. VI. The relationship between the average slope of log (*T*−*T*env) *vs* time, m_1, and relative density, $\overline{\rho}$, of compacted tablets of three different process shear (NAS, 160 Rev sheared, and 640 Rev sheared) powder blends

Table I. Estimated slope of log $(T - T_{env})$ *vs* time at zero porosity, $m_{1,\ 0}$

Cases	$m_{1,\ 0}$	r^2
NAS	0.0399	0.935
160 Rev sheared	0.0366	0.966
640 Rev sheared	0.0330	0.958

Table II. Tensile strength of tablet at zero porosity (σ_0) and critical relative density (ρ_{c,σ_t}) for three different process shear blends

Cases	σ_0(MPa)	ρ_{c,σ_t} (%)	r^2
NAS	4.81	81.4	0.948
160 Rev sheared	3.45	82.2	0.926
640 Rev sheared	2.89	83.0	0.912

compacted tablets from the three cases of powder blends. Table I lists the estimated slope of log $(T - T_{env})$ *vs* time at zero porosity, $m_{1,\ 0}$, of all the three cases. $m_{1,\ 0}$ values are calculated by substituting $\overline{\rho} = 1$ (*i.e.*, $m_{1,\ 0}$ = rate of cooling of tablet at zero porosity) into the linear fit equation in each case shown in Fig. VI.

Figure VII shows that the rate of cooling of tablet at zero porosity, $m_{1,\ 0}$, decreases as the level of process shear increases during formulation process.

Strategy Toward Predicting Tablet Tensile Strength

Higher tablet temperature observed during tablet compaction indicates that there is more heat generated from irreversible deformation on powder particles during the compaction process into the tablet. To further investigate the mechanical properties of the tablets compressed from different process shear conditions, the diametrical compression test is performed using a standard mechanical hardness tester (Dr. Schleuniger Pharmatron, Model 6D, Manchester, NH).

Consider a theoretical model based on percolation theory proposed by Kuentz and Leuenberger (20) to relate tensile strength, σ_t, and relative density, $\overline{\rho}$:

$$\sigma_t = \sigma_0 \left[1 - \left(\frac{1-\overline{\rho}}{1-\rho_{c,\sigma_t}}\right) \exp\left(\overline{\rho} - \rho_{c,\sigma_t}\right)\right] \tag{4}$$

where σ_0 is the tensile strength at zero porosity and ρ_{c,σ_t} is the critical relative density at which σ_t goes to zero.

Relationship between σ_t and $\overline{\rho}$ is normally presented by an exponential form (21–23). This relationship is empirical and does not provide the limiting values of σ_0 and ρ_{c,σ_t} which is needed to implement the model in Eq. (4).

In Fig. VIII, we show the relationship between tablet tensile strength and relative density of compacted tablets of all the three cases of powder blends. As expected, the process shear reduces tablet tensile strength due to the smearing effect of MgSt. Blends with the same formulation but experiencing different level of process shear result in different mechanical properties. This has been reported in the literature, for example in Razavi *et al.* (13) and Pawar *et al.* (24). The diametrical compression test results were fitted to Eq. (4) using the non-linear regression method based on the Trusted-Region algorithm (25). Table II listed tensile strength at zero porosity (σ_0) and critical relative density (ρ_{c,σ_t}) found from Eq. (4) for all three different produced tablets. The results of our finding are consistent with data in Razavi *et al.* (13).

In Fig. IX, from the results in Tables I and II, we present a one-to-one relationship between tensile strength at zero porosity, σ_0, slope of log $(T - T_{env})$ *vs* time at zero porosity, $m_{1,\ 0}$, and critical relative density, ρ_{c,σ_t}, of blends with the same formulation but experienced three different levels of process shear.

$$\sigma_0 = 276.41\ (m_{1,\ 0}) - 6.37 \tag{5}$$

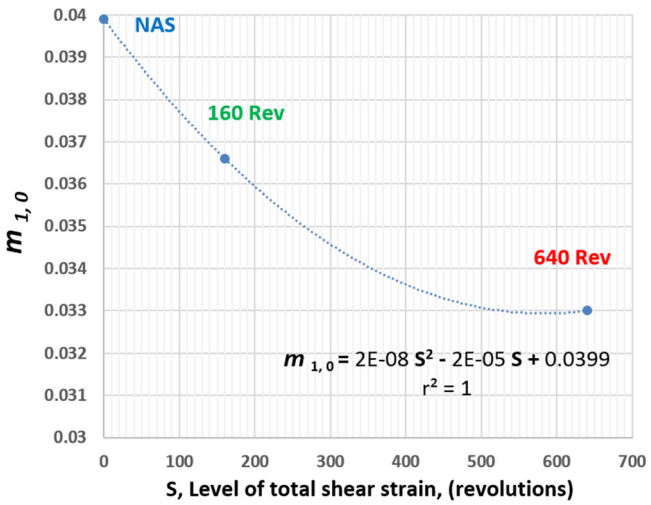

Fig. VII. The relationship between the rate of cooling of tablet at zero porosity, $m_{1,\ 0}$, and the level of total process shear of powder blend experienced during formulation process

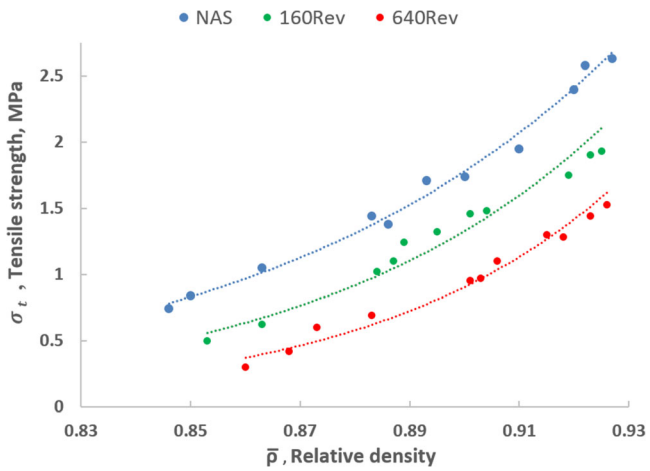

Fig. VIII. The relationship between tablet tensile strength, σ_t, and relative density, $\overline{\rho}$, of compacted tablets of three different total shear strains (NAS, 160 Rev sheared, and 640 Rev sheared) powder blends

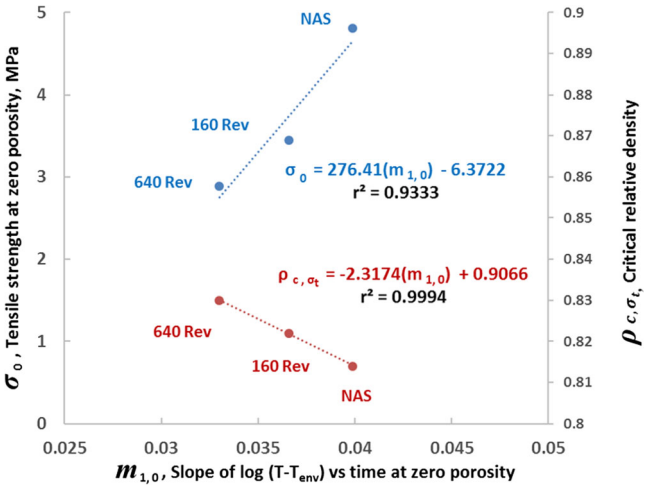

Fig. IX. One-to-one relationship between σ_0, $m_{1,\ 0}$, and ρ_{c,σ_t} of compacted tablets of three different process shear (NAS, 160 Rev sheared, and 640 Rev sheared) powder blends

$$\rho_{c,\sigma_t} = -2.317\ (m_{1,\ 0}) + 0.907 \tag{6}$$

Substituting Eqs. (5) and (6) from experimental data into Eq. (4) yields Eq. (7). We develop the following model toward predicting tablet tensile strength if provided with $m_{1,\ 0}$ and $\overline{\rho}$ information.

$$\sigma_t = [276.41(m_{1,\ 0}) - 6.37]\left[1 - \left(\frac{1-\overline{\rho}}{0.083 + 2.317(m_{1,0})}\right)\exp^{\left(\overline{\rho}+2.317(m_{1,0})-0.907\right)}\right] \tag{7}$$

Figure X shows the prediction of relationship between tablet tensile strength, $\sigma_{t,Eq\ (7)}$, and relative density by applying various rates of cooling of the tablet at zero porosity, $m_{1,\ 0}$, of the range from 0.040 to 0.030 to the model developed in Eq. (7). The range of prediction for unknown sample's tablet tensile strength is presented in Fig. X for relative densities between 0.89 and 0.93 with this nondestructive/noncontact method. As expected, the tensile strength of the tablet decreases as the level of process shear increases. Results in this prediction model are consistent with the data in Fig. VIII using destructive method. The advantage of this PAT prediction model is that it is a nondestructive and noncontact method with real-time instant result of tablet tensile strength without breaking the tablet.

CONCLUSIONS

There is immense potential of using infrared thermography as a nondestructive and noncontact PAT technique for quick screening of the tablet production with pharmaceutical powder subjected to different process shear conditions. We successfully used infrared (IR) measurement system on monitoring the tablet's detail thermal signature during compaction process. The effect of two processing parameters, compaction force and level of process shear**,** were examined. IR measurement of the tablet's rate of cooling, m_1, at *regular regime* was found to be sensitive to the relative density and the level of process shear.

With IR measurement, a correlation between the tablet's rate of cooling at *regular regime* and the tablet's tensile strength is presented. The transient temperature peak exhibits at the center of the tablet. The tablet temperature profile collected by IR after the tablet's ejection from the tablet press provides a unique insight of transient temperature changes. This information can also provide guidance of temperature operating ranges when processing temperature sensitive formulations. The advantage of using the infrared thermography is that this technique is easy to use

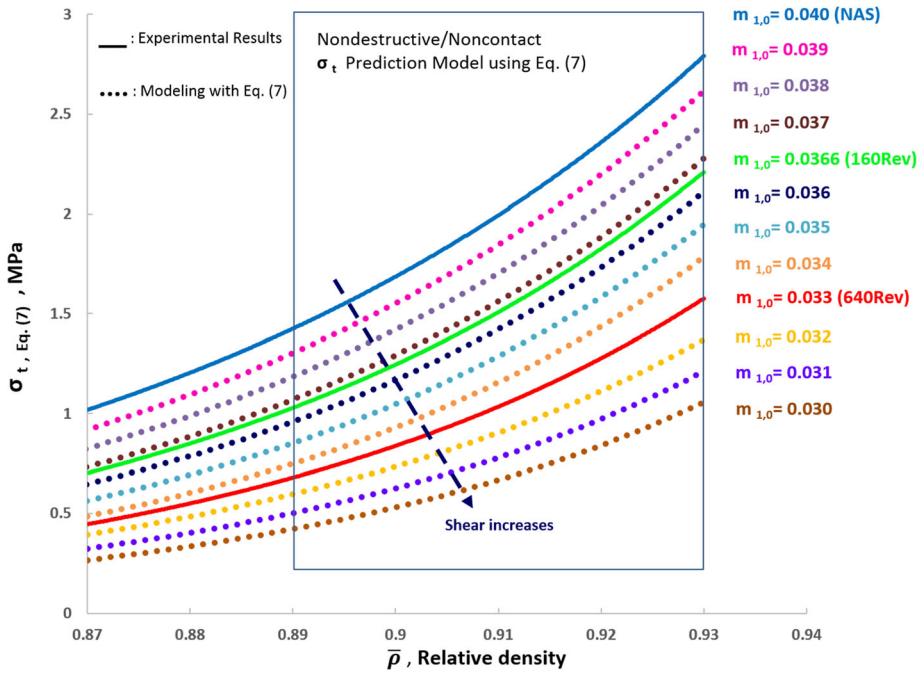

Fig. X. The relationship between tablet tensile strength, $\sigma_{t,\ Eq.\ (7)}$, and relative density, $\overline{\rho}$, by applying tensile strength prediction model using Eq. (7)

and provides a unique thermal signature, $m_{1,\ 0}$, of powder blend's process shear during formulation process toward developing a model to predict tablet tensile strength and it is also a suitable candidate to be placed on/at line as a nondestructive and noncontact PAT tool with instant real-time results.

ACKNOWLEDGEMENTS

The authors wish to thank Professor David Lee of Rutgers New Jersey Agricultural Experiment Station for making it possible to use the infrared camera for this study.

REFERENCES

1. Zavaliangos A, Galen S, Cunningham J, Winstead D. Temperature evolution during compaction of pharmaceutical powders. J Pharm Sci. 2008;97(8):3291–304. https://doi.org/10.1002/jps.21229.
2. Hoag SW, Rippie EG. Thermodynamic analysis of energy dissipation by pharmaceutical tablets during stress unloading. J Pharm Sci. 1994;83(6):903–8.
3. Travers DN, Merriman MP. Temperature changes occurring during the compression and recompression of solids. J Pharm Pharmacol. 1970:Suppl:11S+.
4. Wurster DE, Creekmore JR. Measurement of the thermal-energy evolved upon tablet compression. Drug Dev Ind Pharm. 1986;12(10):1511–28. https://doi.org/10.3109/03639048609065874.
5. Bechard SR, Down GR. Infrared imaging of pharmaceutical materials undergoing compaction. Pharm Res. 1992;9(4):521–8.
6. Ketolainen J, Ilkka J, Paronen P. Temperature-changes during tabletting measured using infrared thermoviewer. Int J Pharm 1993; 92 (1–3):157–166. doi:https://doi.org/10.1016/0378-5173(93)90275-k.
7. Klinzing GR, Zavaliangos A, Cunningham J, Mascaro T, Winstead D. Temperature and density evolution during compaction of a capsule shaped tablet. Comput Chem Eng. 2010;34(7):1082–91. https://doi.org/10.1016/j.compchemeng.2010.04.012.
8. Roueche E, Serris E, Thomas G, Perier-Camby L. Influence of temperature on the compaction of an organic powder and the mechanical strength of tablets. Powder Technol. 2006;162(2):138–44. https://doi.org/10.1016/j.powtec.2005.12.005.
9. Cespi M, Bonacucina G, Casettari L, Ronchi S, Palmieri GF. Effect of temperature increase during the tableting of pharmaceutical materials. Int J Pharm. 2013;448(1):320–6. https://doi.org/10.1016/j.ijpharm.2013.03.014.
10. Pingali KC, Mendez R. Nanosmearing due to process shear—influence on powder and tablet properties. Adv Powder Technol. 2014;25(3):952–9. https://doi.org/10.1016/j.apt.2014.01.016.
11. Pingali KC, Mendez R. Physicochemical behavior of pharmaceutical particles and distribution of additives in tablets due to process shear and lubricant composition. Powder Technol. 2014;268:1–8. https://doi.org/10.1016/j.powtec.2014.07.049.
12. Zhang GGZ, Law D, Schmitt EA, Qiu YH. Phase transformation considerations during process development and manufacture of solid oral dosage forms. Adv Drug Deliv Rev. 2004;56(3):371–90. https://doi.org/10.1016/j.addr.2003.10.009.
13. Razavi SM, Callegari G, Drazer G, Cuitino AM. Toward predicting tensile strength of pharmaceutical tablets by ultrasound measurement in continuous manufacturing. Int J Pharm. 2016;507(1–2):83–9. https://doi.org/10.1016/j.ijpharm.2016.04.064.
14. Mehrotra A, Llusa M, Faqih A, Levin M, Muzzio FJ. Influence of shear intensity and total shear on properties of blends and tablets of lactose and cellulose lubricated with magnesium stearate. Int J Pharm. 2007;336(2):284–91. https://doi.org/10.1016/j.ijpharm.2006.12.013.
15. Pingali KC, Mendez R. Assessing distribution of nanosmears due to mutual interaction of additives in high shear mixing of pharmaceutical blends. Chem Eng Process. 2014;85:248–55. https://doi.org/10.1016/j.cep.2014.09.004.
16. Fell JT, Newton JM. Determination of tablet strength by the diametral-compression test. J Pharm Sci. 1970;59(5):688–91.
17. Luikov AV. Analytical heat transfer theory: academic press; 1968.
18. Isachenko VP, Osipova VA, Sukomel AS. Heat transfer, chapter 39 regular cooling (heating) of bodies. Mir Publisher. 1980:131–9.
19. Sokolovskii RI, Shablygin MV. Application of the quasi-regular cooling regime method to experimental determination of the thermophysical parameters of textile materials. Fibre Chem. 2015;47(2):108–16. https://doi.org/10.1007/s10692-015-9647-4.
20. Kuentz M, Leuenberger H. A new theoretical approach to tablet strength of a binary mixture consisting of a well and a poorly compactable substance. Eur J Pharm Biopharm. 2000;49(2):151–9.
21. Ryshkewitch E. Compression strength of porous sintered alumia and zirconia. J Am Ceram Soc. 1953;36:65–8.
22. Tye CK, Sun CC, Amidon GE. Evaluation of the effects of tableting speed on the relationships between compaction pressure, tablet tensile strength, and tablet solid fraction. J Pharm Sci. 2005;94(3):465–72. https://doi.org/10.1002/jps.20262.
23. Razavi SM, Gonzalez M, Cuitino AM. General and mechanistic optimal relationships for tensile strength of doubly convex tablets under diametrical compression. Int J Pharm. 2015;484(1–2):29–37. https://doi.org/10.1016/j.ijpharm.2015.02.030.
24. Pawar P, Joo H, Callegari G, Drazer G, Cuitino AM, Muzzio FJ. The effect of mechanical strain on properties of lubricated tablets compacted at different pressures. Powder Technol. 2016;301:657–64. https://doi.org/10.1016/j.powtec.2016.05.058.
25. MTALAB. R2016b. Massachusetts: The Math Works Inc. N; 2016.